

Versatile, Fully Automated, Microfluidic Cell Culture System

Rafael Gómez-Sjöberg,[†] Anne A. Leyrat,[†] Dana M. Pirone,[‡] Christopher S. Chen,[‡] and Stephen R. Quake^{*†}

Department of Bioengineering, Stanford University and Howard Hughes Medical Institute, Stanford, California 94305, and Department of Bioengineering, University of Pennsylvania, Philadelphia, Pennsylvania 19104

There is increasing demand for automated and quantitative cell culture technology, driven both by the intense activity in stem cell biology and by the emergence of systems biology. We built a fully automated cell culture screening system based on a microfluidic chip that creates arbitrary culture media formulations in 96 independent culture chambers and maintains cell viability for weeks. Individual culture conditions are customized in terms of cell seeding density, composition of culture medium, and feeding schedule, and each chamber is imaged with time-lapse microscopy. Using this device, we perform the first quantitative measurements of the influence of transient stimulation schedules on the proliferation, osteogenic differentiation, and motility of human primary mesenchymal stem cells.

Cells are cooperatively regulated by numerous signals in their surrounding microenvironment, including diffusible growth factors, the extracellular matrix, and juxtacrine signals from neighboring cells.¹ The temporal and spatial distributions of these signals are tightly controlled and unique to each developmental stage and each organ, affecting all aspects of cell behavior, from proliferation and migration to lineage commitment. It is therefore of interest to reproduce these conditions and control the local environment of in vitro cell culture experiments to the highest possible extent. Robotic fluid handling and microspotting techniques have been employed to produce microarrays of immobilized extracellular matrix (ECM) proteins,² biomaterials,³ and microenvironments composed of mixtures of adsorbed morphogens and extracellular matrix components.⁴ These arrays allowed high-throughput studies of the influence of different immobilized cues on cells but do not address the effects of soluble cues. They require time-dependent stimulation phenomena to be applied to all environments simultaneously, and extracellular factors expressed by the cells are allowed to diffuse between microenvironments.

Microfluidic cell culture platforms^{5–7} combine the advantages of miniaturization and real-time microscopic observation with the ability to pattern cell culture substrates,⁸ to vary the composition of culture medium over space using gradient generators,^{9–11} and to create cell culture conditions that are more physiological than those found in other in vitro systems, in terms of exchange rates of nutrients¹¹ and tunable mechanical stimulation.¹² Microfluidic devices have been successfully used for the long-term culture (up to 4 weeks¹³) of a variety of cells including cell lines,^{9,11,14,15} primary cells such as bovine endothelial cells,¹¹ rat hepatocytes,¹³ rat embryonic neurons,¹⁶ human neural stem cells,¹⁰ and embryonic stem cells.⁹ The devices were used to test different culture conditions for their ability to drive cell growth and proliferation,^{9–11,16} stem/progenitor cell differentiation,^{10,14,15} or to maintain cell function.^{12,13} However, it has been challenging to create devices that both take advantage of microfluidic phenomena and exhibit the combinatorial diversities achieved by microarrays.

We have built an automated cell culture platform around a poly-(dimethylsiloxane) (PDMS) microfluidic chip with 96 individually addressable culture chambers, with a volume of 60 nL each. Individual addressability offers access to a large combinatorial diversity in the experimental space, by allowing one to customize distinct culture environments from chamber to chamber and as a function of time. PDMS is biocompatible and highly permeable to CO₂ and O₂,¹⁷ thereby guaranteeing rapid exchange of these gases between the atmosphere around the chip and the medium in the culture chambers. The microfluidic chip (Figure 1) is

* To whom correspondence should be addressed. E-mail: quake@stanford.edu. Fax: (650) 736-1961.

[†] Stanford University and Howard Hughes Medical Institute.

[‡] University of Pennsylvania.

(1) Scadden, D. T. *Nature* **2006**, *441*, 1075–1079.

(2) Flaim, C. J.; Chien, S.; Bhatia, S. N. *Nat. Methods* **2005**, *2*, 119–125.

(3) Anderson, D. G.; Levenberg, S.; Langer, R. *Nat. Biotechnol.* **2004**, *22*, 863–866.

(4) Soen, Y.; Mori, A.; Palmer, T. D.; Brown, P. O. *Mol. Syst. Biol.* **2006**, *2*, 37.

(5) Khademhosseini, A.; Langer, R.; Borenstein, J.; Vacanti, J. P. *Proc. Natl. Acad. Sci. U.S.A.* **2006**, *103*, 2480–2487.

(6) El-Ali, J.; Sorger, P. K.; Jensen, K. F. *Nature* **2006**, *442*, 403–411.

(7) Breslauer, D. N.; Lee, P. J.; Lee, L. P. *Mol. Biosyst.* **2006**, *2*, 97–112.

(8) Rhee, S. W.; Taylor, A. M.; Tu, C. H.; Cribbs, D. H.; Cotman, C. W.; Jeon, N. L. *Lab Chip* **2005**, *5*, 102–107.

(9) Kim, L.; Vahey, M. D.; Lee, H. Y.; Voldman, J. *Lab Chip* **2006**, *6*, 394–406.

(10) Chung, B. G.; Flanagan, L. A.; Rhee, S. W.; Schwartz, P. H.; Lee, A. P.; Monuki, E. S.; Jeon, N. L. *Lab Chip* **2005**, *5*, 401–406.

(11) Lee, P. J.; Hung, P. J.; Rao, V. M.; Lee, L. P. *Biotechnol. Bioeng.* **2006**, *94*, 5–14.

(12) Leclerc, E.; David, B.; Griscom, L.; Lepioufle, B.; Fujii, T.; Layrolle, P.; Legallais, C. *Biomaterials* **2006**, *27*, 586–595.

(13) Kane, B. J.; Zinner, M. J.; Yarmush, M. L.; Toner, M. *Anal. Chem.* **2006**, *78*, 4291–4298.

(14) Futai, N.; Gu, W.; Song, J. W.; Takayama, S. *Lab Chip* **2006**, *6*, 149–154.

(15) Tourovskaia, A.; Figueroa-Masot, X.; Folch, A. *Lab Chip* **2005**, *5*, 14–19.

(16) Taylor, A. M.; Blurton-Jones, M.; Rhee, S. W.; Cribbs, D. H.; Cotman, C. W.; Jeon, N. L. *Nat. Methods* **2005**, *2*, 599–605.

(17) Merkel, T. C.; Bondar, V. I.; Nagai, K.; Freeman, B. D.; Pinnau, I. *J. Polym. Sci.* **2000**, *38*, 415–434.

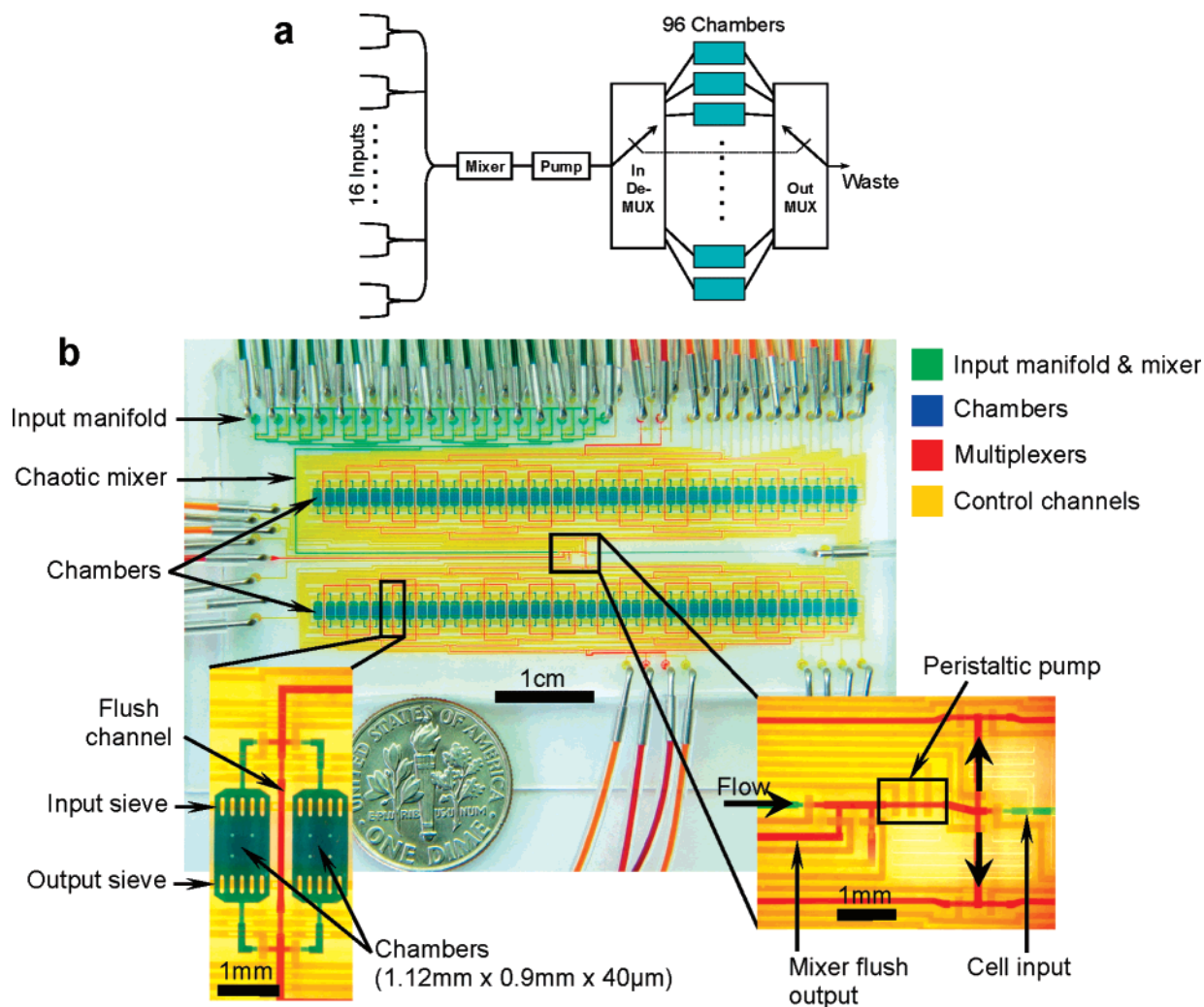


Figure 1. Design of the cell culture chip. (a) Simplified schematic diagram of the fluidic path in the chip (MUX, multiplexer). (b) Annotated photograph of a chip with the channels filled with colored water to indicate different parts of the device. The left inset gives a closer view of two culture chambers, with the multiplexer flush channel in between them. The right inset shows the root of the input multiplexer, with the peristaltic pump, a waste output for flushing the mixer, and the cell input line.

mounted on an automated microscope (Figure S-1, Supporting Information (SI) online), and the system can operate unattended for extended periods of time while providing time-lapse optical imaging of all chambers. The chip was designed to screen the effects of different mixtures of reagents on the behavior of cells over long-term culture. A mixer with 16 different inputs and a multiplexer are used to individually formulate the composition of reagents fed to each chamber and to change this formulation over time with high temporal resolution. Additionally, different cell feeding volumes and frequencies can be chosen for each chamber. It is also possible to customize surface treatments for each chamber by using different ECM protein adhesion coatings at the outset of the experiment. At the end of an experiment, fixing and staining reagents are connected to the inputs to perform fully automated staining procedures. This automation not only reduces the amount of labor involved but also prevents human errors associated with repetitive tasks, while achieving excellent fluid dispensing accuracy. Additionally, the microfluidic platform consumes smaller volumes of reagents than traditional methods. A typical labeling procedure in 96 culture chambers consumes no more than 30 μL of each reagent. Media consumption during

culture varies significantly depending on the specific feeding schedule being used. Frequent changes of media formulations result in increased consumption, due to the need for longer rinsing in between media changes to minimize cross-contamination between chambers. A simple culture with basal medium, renewing 9% of the chamber volume every hour in 96 chambers, consumes ~ 2 mL of medium/day, 98% of which is devoted to rinsing the fluidic paths.

In most culture systems found in the literature, including microfluidic ones, cell seeding density is controlled solely by the concentration of the cell suspension, yielding broad distributions of cell numbers across the culture chambers. This is problematic for cases in which paracrine or juxtacrine signaling between cells affects their behavior, because it introduces higher variability in the local environment. In our system, cell number can be precisely and independently adjusted in each chamber with a single cell suspension concentration by using a sequential loading procedure. The initial cell suspension concentration only affects the precision of seeding density and the amount of time needed to seed the chip. A second cell input can be used to load a different cell sample sequentially without cross-contamination between samples.

EXPERIMENTAL SECTION

More detailed information on the materials and methods used can be found in the Supporting Information.

Chip Design. The chip has 96 rectangular culture chambers with a footprint of 0.9 mm by 1.12 mm and a height of 35–40 μm . This height allows the unrestricted flow of typical rounded human cells in suspension ($\sim 25 \mu\text{m}$ in diameter). Up to 16 different fluid vials can be connected to a chip, to provide surface treatment reagents, culture media, staining reagents, etc. The 16 fluid inputs are connected in a binary tree manifold, with equal fluidic resistance in all branches. The root of the tree is connected to a chaotic mixer (4.8 cm long, 130 μm wide) with a herringbone pattern (46- μm herringbone pitch) on top of the channel,¹⁸ which delivers the fluid to a multiplexer for distribution to any of the 96 chambers, independently or by groups of chambers. An identical multiplexer on the output side routes the flow from each chamber to the waste, keeping the effluent from reaching any of the other chambers by back-diffusion and backflow during changes in the input multiplexer state (valve switching) when one of the chambers is being addressed. An output multiplexer is the most space-efficient way of avoiding these two problems. Every pair of chambers has a flushing line that directly connects the input and output multiplexers, for purging the multiplexer in between medium/reagent changes. These two features minimize cross-contamination across chambers and over time as different fluids are routed to different chambers. Figure S-5a and supporting video 2 (SI) show how the multiplexer allows loading of different solutions in different chambers. An on-chip peristaltic pump composed of three valves in series, located at the root of the multiplexer (Figure 1b), allows injection of very precise doses of culture media or other reagents into each culture chamber. The dosage is controlled by the number of actuation cycles applied to the pump valves, and the flow speed by the frequency at which the valves are switched. Typically, the pump delivers 1% of the chamber volume per cycle, with each cycle lasting 0.15 s. Figure S-5b and supporting video 3 (SI) show how the peristaltic pump is used to inject different doses of reagents into the chambers. As indicated earlier, the chip was fabricated out of PDMS (RTV 615, GE Advanced Materials, Wilton, CT) using the technique of multilayer soft lithography.¹⁹ Details of the chip fabrication procedures can be found in the SI.

Automation. All the valves in the chip are driven by miniature pneumatic solenoid valves (“Ten Millimeter” miniature valves, Numatech Inc., Highland, MI), which are in turn controlled by custom electronic units connected to the USB ports of a computer. The chip is mounted on an automated microscope (Leica DMI6000B, Leica Microsystems GmbH, Wetzlar, Germany) equipped with a motorized X–Y stage, and an environmental chamber for temperature and atmosphere composition control. Custom software developed using Matlab (The Mathworks Inc., Natick, MA) permits fully automated and unattended operation of the system during an experiment. In all the experiments presented here, the cells in the chambers were imaged every hour in phase contrast with 10 \times and 20 \times objectives. Two images were taken per chamber per objective, one of the floor and another of

the ceiling, because cells are typically growing on both surfaces, especially in chambers with high cell densities. During cell culture, all vials with cell culture media or other reagents were pressurized using a mixture of air and 5% CO₂. This pressure drives the flow needed to purge the mixer or the multiplexer with the medium or reagent to be used at each particular time. Driving flows with this positive pressure allows fast fluid exchange and channel rinsing (the peristaltic pump would be too slow for flushing and rinsing), while at the same time avoiding bubbles. Bubbles only enter the chip when the input tubes are first filled, but they quickly disappear by gas diffusion into the PDMS, and they never form during normal operation of the chip. Additionally, positive pressure improves the opening speed of the on-chip valves. Precise injection of fresh medium into the chambers for cell feeding was accomplished by using the on-chip peristaltic pump as explained earlier. The custom control software automatically performed all flow and feeding operations based on user-supplied experimental matrix and feeding schedules. Supporting videos 2 and 3 (SI) show examples of automatic injection of dyed water into different chambers using pressure-driven flow and peristaltically pumped flow, respectively.

Cells. All cells used were human primary mesenchymal stem cells (hMSCs), which are bone marrow stromal cells (nonhematopoietic stem cell population of the bone marrow). They were purchased from Cambrex Corp. (East Rutherford, NJ), which uses the plastic adherence method to enrich the population in cells that are CD105+, CD166+, CD29+, CD44+, CD14-, CD34-, and CD45-, and that are capable of differentiating into chondrocytes, adipocytes, and osteocytes. The cells nevertheless constitute a nonhomogeneous population with purities that vary greatly from batch to batch. They were passed by us a maximum of 4 times before being cultured on-chip. The cells were grown to 90% confluency in T25 flasks using complete growth medium.

Cell Culture Media. All media used for hMSC culture were purchased from Cambrex: Complete growth medium (Catalog No. PT-3001), osteogenic medium (Catalog No. PT-3002 containing ascorbic acid, β -glycerophosphate, and dexamethasone), and adipogenic medium (Catalog No. PT-3004; containing dexamethasone, indomethacin, insulin, and 3-isobutyl-l-methylxanthine).

Surface Treatment of the Chip. At the beginning of each experiment, Pluronic F-127 (Sigma-Aldrich Corp., St. Louis, MO; 0.2% w/w in PBS, filter-sterilized) was incubated for 1 h inside the entire network of flow channels except the culture chambers. This passivated the PDMS surfaces and therefore prevented adsorption of proteins and adherence of the cells to the channels. Then, a sterile solution of fibronectin (Chemicon International Inc., Temecula, CA; 25 $\mu\text{g}/\text{mL}$ in PBS) was incubated in the culture chambers for at least 1 h and then rinsed with growth medium. Fibronectin promoted very efficient cell adhesion to the chamber surfaces.

Cell Suspension Preparation and Loading. When the chip was connected and appropriately treated with pluronic and fibronectin, the cells were trypsinized, centrifuged, counted, and resuspended as a single cell suspension of 500 000 cells/mL. Cells were then seeded on chip at an appropriate seeding density according to the Cambrex protocol (high density for adipogenesis, i.e., 2×10^4 cells/cm²; or low density for osteogenesis, i.e., 6×10^3 cells/cm²). The vial containing the cell suspension was directly

(18) Stroock, A. D.; Dertinger, S. K.; Ajdari, A.; Mezic, I.; Stone, H. A.; Whitesides, G. M. *Science* **2002**, *295*, 647–651.

(19) Unger, M. A.; Chou, H.-P.; Thorsen, T.; Scherer, A.; Quake, S. R. *Science* **2000**, *288*, 113–116.

connected to the cell input port of the chip using a 65- μm -internal diameter polyetheretherketone tubing (PEEK, Upchurch Scientific, Oak Harbor, WA). The suspension was injected into the chip using a differential pressure of 27.6 kPa (4 lbf/in²). Custom software performed the seeding process automatically, based on a user-supplied table specifying the seed population for each chamber. The seeding sequence was as follows: (1) A batch of cells was injected into each chamber by flowing the suspension for a few seconds. (2) Then a phase contrast image was taken for the computer to count the number of injected cells. (3) As the cell loading sequentially cycled through the 96 chambers, cells had time to sediment and attach to the bottom of the chambers (cells attached in less than 5 min). As soon as the cells had attached, an additional batch of cells could be flown through the chambers and the process (1–3) was repeated until the desired seeding density was reached. A cell suspension concentration of 5×10^5 cells/mL resulted in an average of ~ 20 cells/injection. The seeding precision is determined by the cell suspension concentration; lower concentrations give a higher precision at the expense of more injection cycles and, consequently, a longer seeding process. Figure S-2 (SI) shows images of one chamber after injection of each batch of cells and histograms illustrating the high precision with which we can seed the chip, compared with blindly injecting one batch of a suspension into each chamber.

Cell Feeding. Feeding of the cells in the chip was done by pumping a precise amount of fresh medium into each chamber every hour, using the peristaltic pump. In the experiments presented here, all chambers were fed the same amount of medium every hour, at the same flow rate (i.e., same number of pump cycles, same pump actuation frequency). However, the system is flexible enough to allow feeding each chamber with different amounts of media, different schedules, and different pump parameters.

Fixing and Staining. Fixing and staining were performed automatically using the custom chip-control software system. The medium was fully replaced, chamber by chamber, with a solution of 4% w/w paraformaldehyde in PBS. Cycling through the 96 chambers to rinse and make sure no culture medium is left takes ~ 30 min, which corresponds to the incubation time needed to fix the cells. The chambers were then rinsed one by one in the same order using PBS, so that they were all incubated for the same amount of time. Alkaline phosphatase staining was performed using a solution of fast blue RR/naphtol freshly prepared using the components of Sigma Kit 85L2 per manufacturer's instructions. The solution was used within 1 h of preparation by flowing it twice through the chambers, sequentially, for a total incubation time of 1 h in the dark. Oil-red-O (Sigma, 30 mg/mL in 60% 2-propanol) was prepared according to the manufacturer's instructions and filtered using a 0.4- μm filter within 1 h of use. Oil-red-O was very quickly adsorbed by the PDMS, so that the stain disappeared completely within 5 s. It therefore required treating and imaging the chambers one by one (at $10\times$ magnification only). Fluorescent staining of the nuclei was done using DAPI (Invitrogen Corp., Carlsbad, CA, diluted 1:1000 in PBS). Chambers were treated sequentially by groups of 16 and also rinsed with PBS sequentially by groups of 16 for a total incubation time of 7 min/chamber. Von Kossa staining was the last staining performed. The whole chip and the cells were rinsed with deionized water (diH₂O),

followed by 30 min of incubation with a 5% silver nitrate solution in diH₂O under UV radiation, then by 5-min incubation with 5% sodium thiosulfate in diH₂O, and finally they were thoroughly rinsed with diH₂O.

Image Analysis. Counting the number of DAPI-stained nuclei, the number of alkaline phosphatase (AP)-stained cells, and extracting the motility scores were done with custom software written using Matlab, versions 7.0 and 7.2, with Image Processing Toolbox, versions 4.2 and 5.2, respectively (depending on the computer on which the analysis was performed). The motility score was calculated as follows: For each chamber, the floor and ceiling images (phase contrast) from each time point were averaged together and converted to gray scale. Two averaging filters were then applied to the gray scale image to smoothen it, followed by contrast enhancement. Next, all the edges of cells in the enhanced image were found, dilated to increase their thickness, and filtered to remove edge patterns smaller than a manually chosen size. This left a map (a binary image) that contained mostly the outside edges of the cells and some edges corresponding to prominent internal cell features. The edge map at each time point was compared to that of the previous time point to compute the total number of edge pixels that changed, both from 0 to 1 and from 1 to 0. The motility score is then defined as the total number of edge pixels that changed, divided by the total number of pixels in the edge map. This normalization eliminates changes in the edge map that results from cell proliferation and makes the score have values between 0 and 2. More detailed descriptions of the algorithms can be found in the SI.

Statistical Analyses. All statistical analyses were performed with the Matlab Statistics Toolbox version 5.0. Detailed descriptions of the analyses can be found in the SI.

RESULTS AND DISCUSSION

We demonstrated the ability of this culture platform to sustain proliferation and stimulate differentiation of hMSCs. Standard differentiation media were used to induce osteogenic and adipogenic differentiation of hMSCs. Culture chambers were treated with fibronectin and then seeded at appropriate densities (20 000 cells/cm² for adipogenesis, 6000 cells/cm² for osteogenesis). Cell proliferation was assessed by counting cells at the beginning and end of the experiment. Osteogenic differentiation was assessed by counting the percentage of cells stained positively for AP activity. AP is a bone matrix enzyme whose expression is upregulated during early osteogenic differentiation and is routinely used as a marker of osteogenesis.^{20,21} Adipogenesis was assayed by staining the lipid droplets using Oil Red O. Proliferation and differentiation rates obtained on chip were comparable to values found in parallel control assays performed in standard tissue culture and in the literature.²² Figure S-3 (SI) shows cells stained for AP activity and for lipid droplets in the chambers. Because AP activity is only indicative of, and not specific to, osteogenesis, we also assayed for calcium deposition in osteogenic culture conditions using Von Kossa's method. By day 9 of continuous stimulation, 88% of the stimulated chambers stained very positive

(20) Aronow, M. A.; Gerstenfeld, L. C.; Owen, T. A.; Tassinari, M. S.; Stein, G. S.; Lian, J. B. *J. Cell. Physiol.* **1990**, *143*, 213–221.

(21) Aubin, J. E.; Turksen, K. *Microsc. Res. Tech.* **1996**, *33*, 128–140.

(22) McBeath, R.; Pirone, D. M.; Nelson, C. M.; Bhadriraju, K.; Chen, C. S. *Dev. Cell* **2004**, *6*, 483–495.

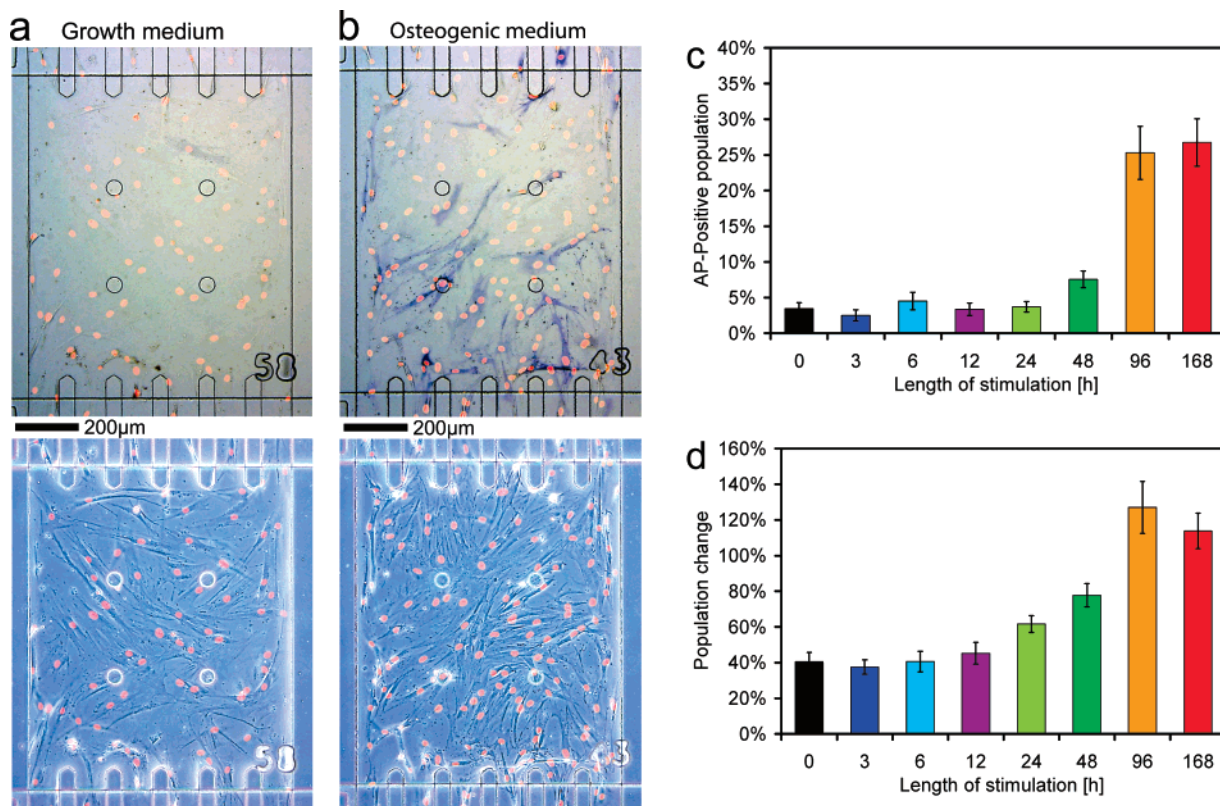


Figure 2. Effect of osteogenic stimulation on differentiation and proliferation during transient stimulation. Bright field and phase contrast microscopic observations (false-color DAPI image superimposed) of representative chambers of (a) the control group fed only with growth medium for 168 h and (b) the group stimulated for 96 h with osteogenic medium. In (a), the initial cell number is 59 and the final cell number is 83. In (b), the initial cell number is 52 and the final cell number is 160. (c) Average fraction of cells that differentiated in each stimulation group, as indicated by the number of cells that stain positive for alkaline phosphatase activity. (d) Average relative change in the number of cells over the whole incubation time for each stimulation group. Error bars correspond to the standard error of the means ($n = 12$).

for calcium deposition, 8% stained weakly positive, 4% contained only dead cells, and none had negative staining (Figure S-4, SI). In contrast, control chambers fed with only the nondifferentiating growth medium showed no calcium deposition. These findings demonstrate the ability of the cell culture chip to support long-term studies, such as stem cell differentiation, and highlight the versatility of the approach to automate common culturing and assaying procedures. These include depositing extracellular matrix coatings, seeding cells, and exchanging media, staining solutions, and rinsing buffers.

Because cells consume components and also introduce new factors into the culture medium, the medium changes over time. Although controlling a variety of feeding schedules is cumbersome in standard culture, the automation within our cell culture chip allows one to easily and precisely study the culture medium exchange rates, the conditions of fluid flow through the culture chambers, and to explore different types of temporal gradients in the environmental conditions. To illustrate this capability, we studied how long of an osteogenic stimulus is required to induce hMSC differentiation, by examining the effect of eight different durations of osteogenic stimulation (0, 3, 6, 12, 24, 48, 96, or 168 h following an initial phase of 12 h in the presence of growth medium) on the osteogenic differentiation and motility of hMSCs. Initial tests of on-chip hMSC differentiation indicated some heterogeneity in results between chambers. Each duration of stimulation was therefore run in 12 chambers, each seeded with 60 cells, yielding an initial total number of ~ 720 cells per condition.

All chambers were fed growth medium for the first 12 h after cell seeding. After this, the growth medium in all chambers assigned to stimulation groups was fully replaced by fresh osteogenic medium using a low flow rate produced by pressure-driven flow. When the stimulation period of each group ended, the medium in those chambers was fully replaced with growth medium by pressure-driven flow. Outside of the medium switching periods, all chambers were fed either growth or osteogenic medium by replacing 40% of the chamber volume every hour using the peristaltic pump. This renewal rate is high enough to reduce the effects of paracrine signaling and make cell behavior depend mainly on the factors provided in the medium. Although faster renewal rates would suppress paracrine signaling completely, our previous tests had indicated that they can inhibit cell growth and differentiation. We therefore first confirmed that this exchange rate was in the range that could support hMSC differentiation using the classical end-point assays based on AP staining (Figure 2). All chambers were exposed to the same flow conditions during routine feeding with the peristaltic pump, so that any effects that flow-induced shear stress could have on differentiation are the same across all conditions, including the control group. The maximum shear stress on the cells in the osteogenic groups during medium replacement was on the order of 0.05 N/m^2 (with a flow rate of 6.5 nL/s). This shear stress is close to 1 order of magnitude smaller than the minimum level that has been shown to affect differentiation or proliferation when applied continu-

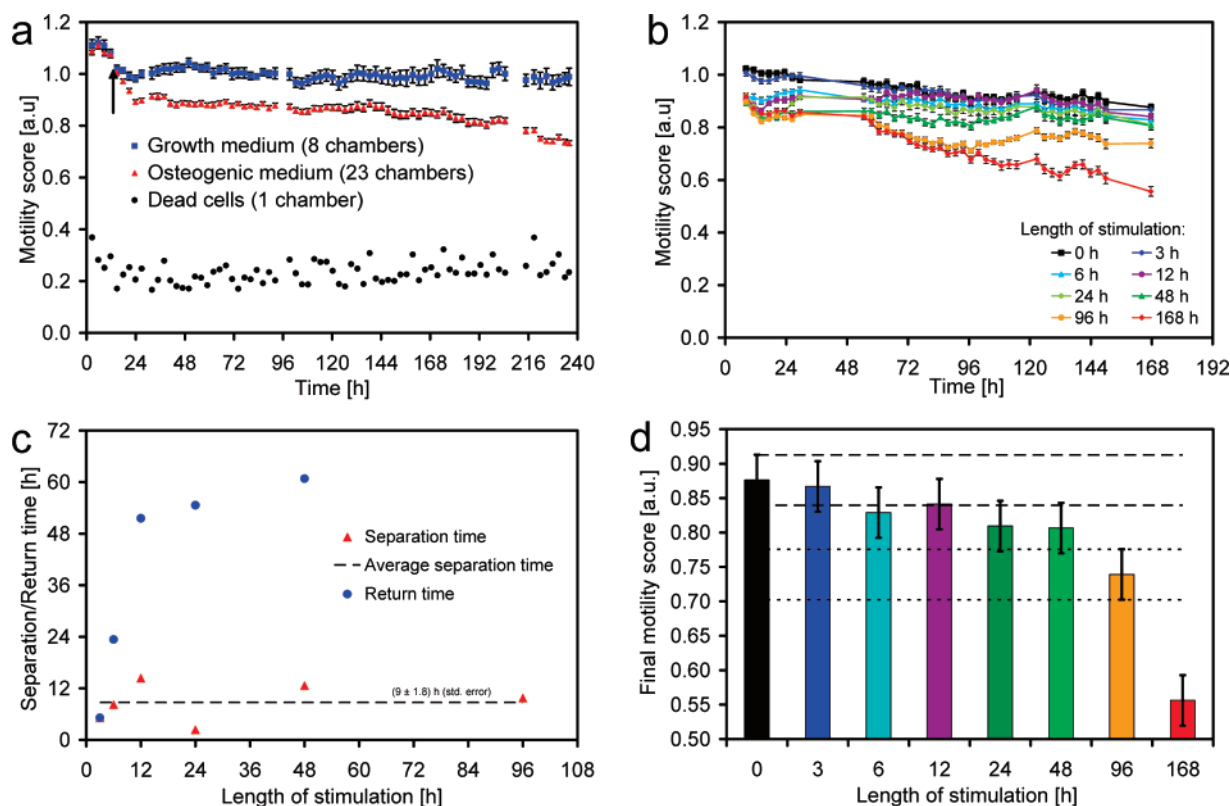


Figure 3. Effects of osteogenic stimulation on cell motility. (a) Plot of motility scores over time from continuous stimulation (control chambers, in blue, were fed only with growth medium; stimulated chambers, in red, were fed with osteogenic medium for 9 days). The black arrow indicates the point where the medium was switched from growth to osteogenic. The motility scores from a chamber with 42 dead cells are included for comparison (black curve). Each point corresponds to an average over three scores (three consecutive images). Error bars correspond to the standard error of the means, given the number of samples per group n shown in the legend. Times are relative to the start of the incubation. (b) Evolution of motility over time for 8 different lengths of transient stimulation (12 chambers per schedule). Each point corresponds to an average over three images, taken 1 h apart. Lines connecting the points were added to guide the eye. Error bars correspond to the standard error of the means ($n = 12$). (c) Separation and return times, measured from the end of stimulation, plotted as a function of the length of osteogenic stimulation. The average separation time is 9 ± 1.8 h (standard error). (d) Comparison of final motilities (final points in b) across the 8 transient stimulation schedules. Error bars indicate 95% confidence level intervals for multiple comparisons, derived using the Tukey honestly significant difference method. Dotted lines are extensions of the 95% confidence level intervals of the 0- and 96-h groups, to aid in comparisons between groups.

ously,^{23,24} and the cells were exposed to it for only 6 s twice during a 7-day period.

Representative microscopic observations of the control group (Figure 2a) and the group stimulated for 96 h (Figure 2b) obtained in phase contrast and bright field illustrate the ability of the cells to proliferate and differentiate. Panels c and d in Figure 2 show that while proliferation and differentiation both increase with the length of osteogenic stimulation, 96 h of osteogenic media causes a substantial increase in responses that is similar to continuous (168 h) stimulation. These results suggest that hMSCs need a minimum of 4 days of stimulation to fully commit to differentiation into the osteogenic lineage.

We further characterized the influence of the length of stimulation by analyzing the overall motility of the cells. Time-lapse imaging (supporting video 1, SI) revealed that overall cell motility decreased in chambers where cells were stimulated with osteogenic medium. To quantify the evolution of cell motility over time, we developed a scoring system that indicates the amount of cell motion over the whole chamber at each time point (see SI).

(23) Kreke, M. R.; E., M.; Goldstein, A. S. *Tissue Eng.* **2004**, *10*, 780–788.

(24) Riddle, R. C.; Taylor, A. F.; Genetos, D. C.; Donahue, H. J. *Am. J. Physiol. Cell Physiol.* **2005**, *290*, 776–784.

We compared the motility of the cells stimulated continuously for 9 days to the motility of nonstimulated cells (Figure 3a). The two groups of chambers begin with identical behavior, which is characterized by an initial phase of high motility as the cells distribute themselves over the chamber and spread in place, followed by a continuous decline in motility as the cells reach stable configurations. Then, 18 h after the start of incubation with differentiation medium (sixth data points in Figure 3a), the mean motilities of the two groups become significantly different ($p = 0.0146$ by one-way ANOVA, 8 chambers in the growth group, 23 in the osteogenic group). The nonstimulated cells settle into an almost constant level of motility for the duration of the experiment, while the stimulated ones exhibit a continuous decrease in motility (with an abrupt change of slope 24 h after the start of incubation). The final means of the two groups are different by 26% (with $p = 3.4 \times 10^{-11}$). To confirm that the motility score measures the real motion of the cells, Figure 3a also shows the motility curve from a chamber with dead cells, which does not exhibit any pattern. The nonzero signal produced by dead cells is mainly the result of small changes in illumination and focus between frames and, to a lesser extent, jitter in the automated microscope stage.

Figure 3b shows the motility scores obtained for the eight different stimulation schedules of the transient stimulation experiment. The curve obtained for the positive control (group stimulated for 168 h) and the negative control (growth medium only) confirms the trends observed in the continuous stimulation experiment. Some time after the stimulation is stopped the motility score diverges from that of the positive control, thereby showing the sensitivity of this measurement in detecting cell reaction to a change in the chemical environment. We define "separation time" as the time when the average motility of a given group becomes significantly (statistically) different from the motility of the positive control. Separation time, measured from the end of stimulation, seems to be independent of the length of stimulation, with an average value of (9 ± 1.8) h (standard error) (Figure 3c). This indicates that motility responds to the removal of osteogenic stimulation with a delay that is independent of the length of stimulation. After stimulation is stopped, the cells stimulated for less than 96 h progressively recover a level of motility that becomes statistically indistinguishable from that of the unstimulated control group. The motion score of the group stimulated for 96 h remains significantly different from the negative and the positive controls (Figure 3d). Consequently, we can define a "return time" for the groups stimulated for less than 96 h, which corresponds to the time necessary for each group to return to the same motility as the negative control, after stimulation is stopped. In contrast to the separation time, the return time, measured from the end of stimulation, is a nonlinear function of the length of stimulation (Figure 3c). More details on the extraction of the separation and return times can be found in the SI. Further study will be required in order to elucidate the details

of the dynamics involved in these changes in motility, as well as to determine if there is a causal relationship between induction of differentiation and decrease in motility of the stem cells.

CONCLUSIONS

In summary, we have built a fully automated microfluidics-based platform for mammalian cell culture that provides unattended stimulation of the cells using complex time-varying schedules, and in situ mixing of media and reagents, while allowing time-lapse microscopic imaging. We have demonstrated the basic functionality of the system by studying the relationship between exposure to osteogenic differentiation media and motility of primary human mesenchymal stem cells. We have performed the first measurements of the effect of osteogenic differentiation factors on cell motility and have demonstrated that these effects are reversible and exhibit interesting dynamics.

ACKNOWLEDGMENT

This work was supported by a National Institutes of Health Director's Pioneer Award (DP1 OD000251) and the National Institute of General Medical Sciences (GM74048). R.G.-S. and A.A.L. contributed equally.

SUPPORTING INFORMATION AVAILABLE

Additional information as noted in the text. This material is available free of charge via the Internet at <http://pubs.acs.org>.

Received for review June 20, 2007. Accepted September 7, 2007.

AC071311W